

Steady-state and transient photocurrents of As-S-Sb-Te amorphous thin films

O. V. Iaseniuc*, M. S. Iovu

Institute of Applied Physics, Moldova State University, 5 Academiei str., MD2028, R. Moldova

In the present work some nanostructured quaternary chalcogenides of the As-S-Sb-Te system have been investigated by a photoelectric method. The spectral distribution of steady-state photocurrent $I_{ph}=(\lambda)$ and the relaxation curves of photocurrent $I_{ph}=(t)$ were registered at positive and negative polarity of the applied voltage to the top Al illuminated electrode. In the spectral distribution of steady-state photocurrent, for the amorphous thin films $As_{1.17}S_{2.7}Sb_{0.83}Te_{0.40}$, $As_{1.04}S_{2.4}Sb_{0.96}Te_{0.60}$, $As_{0.63}S_{2.7}Sb_{1.37}Te_{0.30}$, and $As_{0.56}S_{2.4}Sb_{1.44}Te_{0.60}$ in the wavelength range $\lambda=0.50\div 0.92\ \mu m$ (2.48 \div 1.35 eV) some maxima were detected, which are the result of the presence of binary clusters As_2S_3 , Sb_2S_3 and Sb_2S_3 . The photovoltaic method was used to obtain the value of the band gap width, which was about $E_g=1.41\ eV$.

(Received May July 7, 2023; Accepted October 10, 2023)

Keywords: Amorphous thin films, Steady-state photoconductivity, Transient photocurrents

1. Introduction

Nanostructured chalcogenide semiconductor alloys of quaternary system As-S-Sb-Te (with the main average coordination number $Z=2.40$, containing elements of V (As, Sb) and VI (S, Te) groups), are interesting and important from the point of view of assessing their physical properties as well as for determining the scope of technical application, such as IR optical elements, diffractive optics, holography, photonic and gas sensors, etc. [1-2]. These As_2S_3 , Sb_2S_3 , and Sb_2Te_3 semiconductors and its ternary and quaternary compounds are the most intensively studied chalcogenide glasses because of its ease of formation, its excellent infrared transmission and its resistance to atmospheric conditions and chemical stability. Even though As and Sb belong to the same group of the periodic table, As_2S_3 , Sb_2S_3 , and Sb_2Te_3 do not display the same glass forming tendency. Addition of As_2S_3 to Sb_2S_3 enhances the glass forming ability and glasses in the mixed As-S-Sb system can be formed [3]. The three-dimensional network of As_2S_3 glassy is built of trigonal pyramidal units $AsS_{3/2}$, which are interconnected through As-S-As bridges. The basic structural units of Sb_2S_3 glassy are the trigonal pyramidal arrangement $SbS_{3/2}$ bonded to each other by S atoms [4]. The crystal structure of Sb_2Te_3 exhibits the layered atomic arrangement in the rhombohedral structure, which consists of three quintuplet layers (QLs) and each quintuplet layer contain five atoms in the order of $Te^1-Sb-Te^2-Sb-Te^1$ [5].

Some photoelectrical properties of $(Sb_{15}As_{30}Se_{55})_{100-x}Te_x$ ($0\leq x\leq 12.5$ at.%) thin films were investigated in [6]. It was shown that with increasing of Te concentration in the alloys, the maximum of photoconductivity is shifted towards red region of the spectra from 800 nm to 950 nm. In [7] the results on the spectral distribution of steady-state photocurrent in bulk $As_{11.2}S_{48.0}Sb_{28.8}Te_{12.0}$ and $As_{20.8}S_{48.0}Sb_{19.2}Te_{12.0}$ alloys at different applied voltage were reported. In the spectral distribution of the stationary photocurrent $I_{pc}=f(\lambda)$ for $As_{11.2}S_{48.0}Sb_{28.8}Te_{12.0}$ and $As_{20.8}S_{48.0}Sb_{19.2}Te_{12.0}$ nanostructured semiconductors was observed a maximum situated around $\lambda=0.96\ \mu m$ ($h\nu=1.29\ eV$). Beside that for the $As_{11.2}S_{48.0}Sb_{28.8}Te_{12.0}$ semiconductor an additional shoulder is situated around $\lambda=0.76\ \mu m$ ($h\nu=1.63\ eV$), and for $As_{20.8}S_{48.0}Sb_{19.2}Te_{12.0}$ semiconductor the additional shoulder is situated around $\lambda=0.68\ \mu m$ ($h\nu=1.82\ eV$).

The present work reports experimental results concerning the steady-state and transient photocurrents of the $As_{1.17}S_{2.7}Sb_{0.83}Te_{0.40}$, $As_{1.04}S_{2.4}Sb_{0.96}Te_{0.60}$, $As_{0.63}S_{2.7}Sb_{1.37}Te_{0.30}$, and $As_{0.56}S_{2.4}Sb_{1.44}Te_{0.60}$, semiconductor amorphous thin films. Semiconductors containing elements

* Corresponding author: oxana.iaseniuc@gmail.com

<https://doi.org/10.15251/CL.2023.2010.725>

As, S, Sb, and Te are high photosensitive amorphous materials, and widely are used as photodetectors and recording media of optical information. On the other hand, semiconductors containing elements Sb and Te are well known as "ovonic" materials for volatile memory. We show more complicated materials containing As, S, Sb, Te in order to combine these two advantages using a single composition.

2. Experimental results and discussions

The quaternary semiconductor of the As-S-Sb-Te system was prepared from the elements of 6N purity (As, Sb, S, Te) by conventional melt quenching method. In order to simplify the synthesis procedure initially were prepared the binary components As_2S_3 , Sb_2S_3 , Sb_2Te_3 , and the ternary alloys $(\text{As}_2\text{S}_3)_{0.35}(\text{Sb}_2\text{S}_3)_{0.65}$, $(\text{As}_2\text{S}_3)_{0.65}(\text{Sb}_2\text{S}_3)_{0.35}$. The initial chemical components were weighed, placed and mixed in quartz ampoules which then were evacuated up to pressure of $P \sim 10^{-5}$ Torr and sealed. At last, the mixtures were melted at 850-900 °C in rocking furnace during 10 hours for homogenization, and then quenched at the room temperature.

The experimental samples for photoelectric measurements have a "sandwich" configuration with two Al-electrodes. The top Al-electrode was semitransparent for the incident light. Thickness of the samples was about $d \approx 0.2 \div 0.5 \mu\text{m}$. The dark current, current under light exposure, the spectral distribution of stationary photocurrent $I_{ph} = f(\lambda)$, and the transient photocurrents were registered in the constant current conditions, using the electrometer amplifiers U5-11, with the error less than $\pm 1.0 \%$. The wavelength was adjusted by the spectrophotometer SPM-2, the intensity has been varied with the neutral filters HC. All experiments were performed at room temperature ($T \approx 20 \text{ }^\circ\text{C}$).

Some experimental results on XRD, EDS and micro-Raman spectroscopy of As-S-Sb-Te system as bulk, powder and thin film samples were reported in [7, 8]. It has been shown that the quaternary compounds $\text{As}_{1.17}\text{S}_{2.7}\text{Sb}_{0.83}\text{Te}_{0.40}$, $\text{As}_{1.04}\text{S}_{2.4}\text{Sb}_{0.96}\text{Te}_{0.60}$ and $\text{As}_{0.56}\text{S}_{2.4}\text{Sb}_{1.44}\text{Te}_{0.60}$ have a polycrystalline structure, and the other one $\text{As}_{0.63}\text{S}_{2.7}\text{Sb}_{1.37}\text{Te}_{0.30}$ has an amorphous structure with broad peaks specific for non-crystalline materials. Studying of photoelectric properties allows obtaining information about the generation and recombination processes in chalcogenide semiconductors [7-10].

Fig. 1 – 4 represent experimental results on spectral distribution of steady-state photocurrent $I_{ph} = f(\lambda)$ with positive of the applied voltage to the top Al illuminated electrode $U = 1 \text{ V}$, for the maximum photocurrent value (1) (at the moment of turning on the light, the I_{ph} photocurrent reaches its maximum value) and for the stationary value (2) (when the photocurrent relax in time to its stationary value); dependence of the transient photocurrent on the time $I_{ph} = f(t)$ at different wavelengths (b) (λ , nm: 1 - 420, 2 - 540, 3 - 700, 4 - 740) and dependence of the transient photocurrent on time at different light intensities $I_{ph} = f(F)$ (c) (F , %: 1 - 1.5, 2 - 15, 3 - 20, 4 - 100.) for amorphous thin films: $\text{As}_{1.17}\text{S}_{2.7}\text{Sb}_{0.83}\text{Te}_{0.40}$ (thickness is $L = 0.135 \mu\text{m}$), $\text{As}_{1.04}\text{S}_{2.4}\text{Sb}_{0.96}\text{Te}_{0.60}$ (thickness is $L = 0.54 \mu\text{m}$), $\text{As}_{0.63}\text{S}_{2.7}\text{Sb}_{1.37}\text{Te}_{0.30}$ (thickness is $L = 0.27 \mu\text{m}$) and $\text{As}_{0.56}\text{S}_{2.4}\text{Sb}_{1.44}\text{Te}_{0.60}$, (thickness is $L = 0.18 \mu\text{m}$).

For both curves in the spectral distribution for compound $\text{As}_{1.17}\text{S}_{2.7}\text{Sb}_{0.83}\text{Te}_{0.40}$ we observe three definite maxima: at $\lambda = 540 \text{ nm}$, $\lambda = 600 \text{ nm}$ and $\lambda = 920 \text{ nm}$; for $\text{As}_{1.04}\text{S}_{2.4}\text{Sb}_{0.96}\text{Te}_{0.60}$ one broad peak at about 600 nm; for $\text{As}_{0.63}\text{S}_{2.7}\text{Sb}_{1.37}\text{Te}_{0.30}$ we observe some maximums situated at $\lambda = 520 \text{ nm}$, 570 nm , 600 nm , 710 nm , and around 700 nm and for $\text{As}_{0.56}\text{S}_{2.4}\text{Sb}_{1.44}\text{Te}_{0.60}$ one broad peak at about 500 nm. These maxima may be associated with the presence of As_2S_3 , Sb_2S_3 and Sb_2Te_3 clusters in the structure of the studied samples. It was also observed that, difference between maximum and stationary values of photocurrent for all compounds depends on the wavelength value as illustrated in Fig. 1 – 4b). Besides that, difference between the maximum and stationary values of photocurrent also depends on the excitation light intensity F (%) for all investigated compounds: 1 - 1.5, 2 - 15, 3 - 20, 4 - 100 ($\lambda_{exc} = 540 \text{ nm}$) (Fig 1c).

In addition, it was measured photocurrent at the negative applied voltage to the top Al illuminated electrode. As an example, the Fig. 5 shows the spectral distribution of steady-state photocurrent for amorphous thin film $\text{As}_{1.04}\text{S}_{2.4}\text{Sb}_{0.96}\text{Te}_{0.60}$, both for the maximum (1) and stationary (2) photocurrent value at the negative applied voltage to the top Al illuminated electrode. The other compositions exhibit similar behavior of spectral curves.

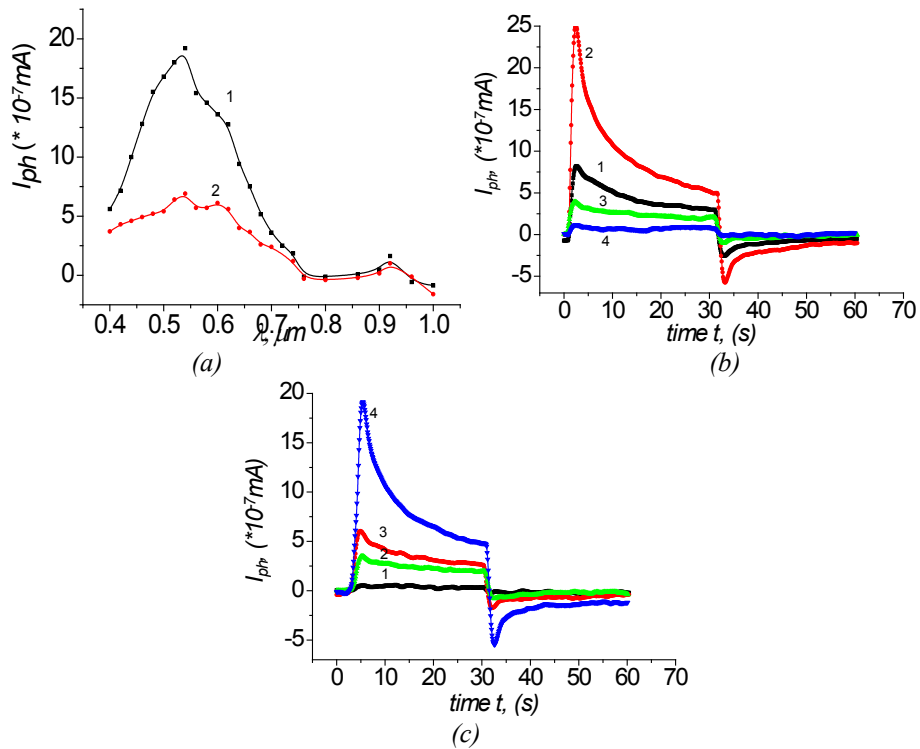


Fig. 1. Spectral distribution of steady-state photocurrent for amorphous thin film $As_{1.17}S_{2.7}Sb_{0.83}Te_{0.40}$ (both for the maximum (1) and stationary (2) photocurrent value (a); dependence of the transient photocurrent on the time at different wavelengths (b) and dependence of the transient photocurrent on time at different light intensities (c).

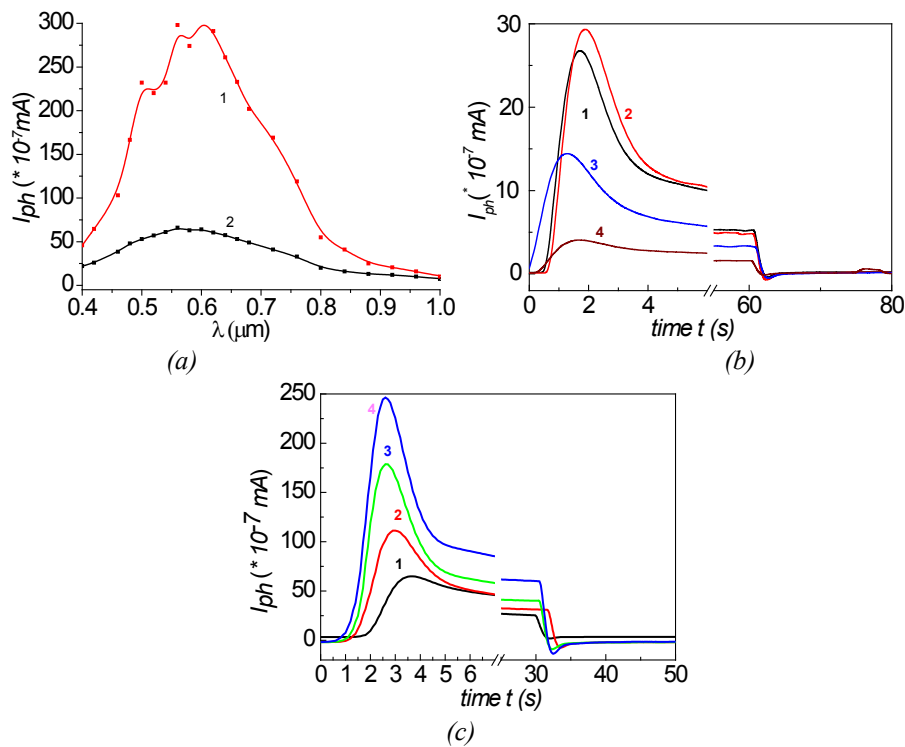


Fig. 2. Spectral distribution of steady-state photocurrent for amorphous thin film $As_{1.04}S_{2.40}Sb_{0.96}Te_{0.60}$ (both for the maximum (1) and stationary (2) photocurrent value (a); dependence of the transient photocurrent on the time at different wavelengths (b) and dependence of the transient photocurrent on time at different light intensities (c).

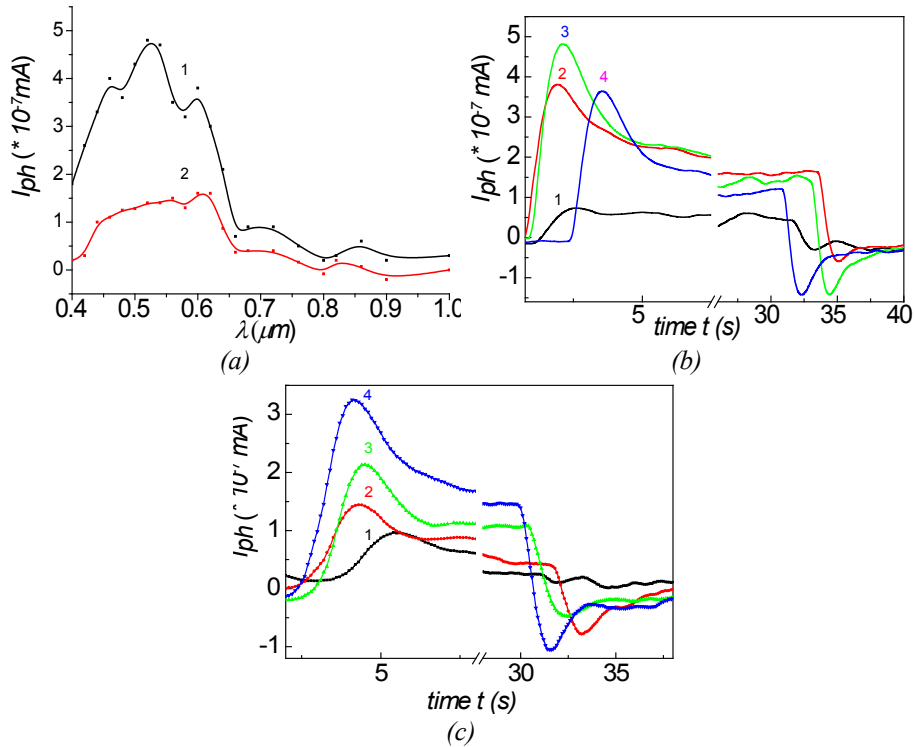


Fig. 3. Spectral distribution of steady-state photocurrent for amorphous thin film $As_{0.63}S_{2.70}Sb_{1.37}Te_{0.30}$ (both for the maximum (1) and stationary (2) photocurrent value (a); dependence of the transient photocurrent on the time at different wavelengths (b) and dependence of the transient photocurrent on time at different light intensities (c).

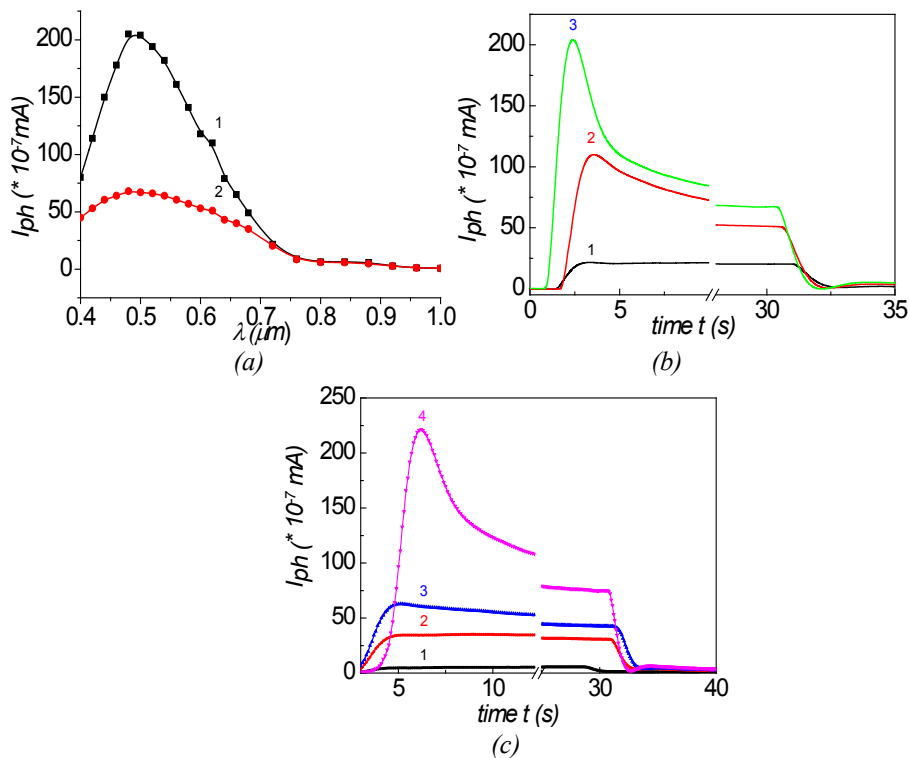


Fig. 4. Spectral distribution of steady-state photocurrent for amorphous thin film $As_{0.56}S_{2.40}Sb_{1.44}Te_{0.60}$ (both for the maximum (1) and stationary (2) photocurrent value (a); dependence of the transient photocurrent on the time at different wavelengths (b) and dependence of the transient photocurrent on time at different light intensities (c).

It is well known that photocurrent I_{ph} in amorphous semiconductor materials is proportional to the absorption coefficient α , quantum efficiency β , drift mobility μ_d , and life time τ .

$$I_{ph} \sim \frac{1 - e^{-\alpha d}}{L} \beta \mu_d \tau \quad (1)$$

In the weak absorption region at the energy photons $h\nu$ less than the optical band gap E_g , ($h\nu \leq E_g$ long wavelength region), the photocurrent I_{ph} is described by the absorption coefficient α .

$$I_{ph} \sim \beta \alpha \mu_d \tau \quad (2)$$

The behavior of the photocurrent after reaching the maximum value on the spectral distribution curves in the high-energy region is caused by an increase in the surface recombination rate. The spectral distribution of the stationary photocurrent $I_{phc} = f(\lambda)$ for $As_{0.56}S_{2.40}Sb_{1.44}Te_{0.60}$ and $As_{1.04}S_{2.40}Sb_{0.96}Te_{0.60}$ bulk nanostructured semiconductors at different applied voltages ($U=10\div 300$ V) and in the wavelength range from $0.4\div 1.3$ μm was reported in [7]. It was established that in all photocurrent spectral distributions the maximum photosensitivity is situated around $\lambda=0.96$ μm ($h\nu \approx 1.29$ eV). Besides that, in these spectral distributions of the stationary photocurrent an additional shoulder appears around $\lambda=0.76$ μm ($h\nu \approx 1.63$ eV) for $As_{0.56}S_{2.40}Sb_{1.44}Te_{0.60}$ and around $\lambda=0.68$ μm ($h\nu \approx 1.82$ eV) for the $As_{1.04}S_{2.40}Sb_{0.96}Te_{0.60}$ semiconductors. The presence of a second maximum in the spectral distribution of the photocurrent, taking into account X-ray diffraction data, may be due to the presence of nanostructured Sb_2S_3 and Sb_2Te_3 structural units in alloys [7].

In our case, for the amorphous thin films of As-S-Sb-Te system the maximum of the stationary photocurrent at positive polarity of the applied voltage to the top Al illuminated electrode is situated in the region of the photon energy of $h\nu \approx 2.66$ eV ($\lambda=0.60$ μm) for $As_{0.63}S_{2.70}Sb_{1.37}Te_{0.30}$ and $As_{1.04}S_{2.40}Sb_{0.96}Te_{0.60}$, at $h\nu \approx 2.30$ eV ($\lambda=0.54$ μm) for $As_{1.17}S_{2.70}Sb_{0.83}Te_{0.40}$ and at $h\nu \approx 2.38$ eV ($\lambda=0.52$ μm) $As_{0.63}S_{2.70}Sb_{1.37}Te_{0.30}$. Some additional maximum are observed at $h\nu=1.35$ eV ($\lambda=0.92$ μm) $As_{1.17}S_{2.70}Sb_{0.83}Te_{0.40}$ and $h\nu=2.64$ eV ($\lambda=0.47$ μm), $h\nu=1.75$ eV ($\lambda=0.71$ μm), $h\nu=1.44$ eV ($\lambda=0.86$ μm) $As_{0.63}S_{2.70}Sb_{1.37}Te_{0.30}$. These maximums can be associated with the presence of amorphous and nanocrystalline phases with the structural units As_2S_3 , Sb_2S_3 , and Sb_2Te_3 , as was demonstrated by the results of XRD and micro-Raman experiments [8]. These particularities in the spectral distribution curves of steady-state photocurrent may be generated by the specific structure of the investigated materials, as well as by the contact phenomena between the interfaces of the amorphous material with the metallic electrode [1, 11]. It was demonstrated, that at the interface between the metallic electrode (Al) and chalcogenide amorphous thin film (Sb_2S_3 , As_2S_3 , As_2Se_4) exists a potential barrier (φ_b), the height of which depends on the nature of the metal and amorphous material ($\varphi_b = 0.35\div 0.65$ eV). Besides that, the different shape of the spectral distribution of the steady-state photocurrent curves at positive polarity of the applied voltage can be governed by the drift of non-equilibrium carriers through the volume of the sample in the conditions of the multiple trapping on the localized states in the band gap of the disordered material [12].

The kinetics of transient photocurrents in amorphous As-based chalcogenide thin films was widely reported and discussed in [9, 12-16]. As in previous articles, for the amorphous thin films $As_{1.17}S_{2.70}Sb_{0.83}Te_{0.40}$, $As_{1.04}S_{2.40}Sb_{0.96}Te_{0.60}$, $As_{0.63}S_{2.70}Sb_{1.37}Te_{0.30}$, and $As_{0.56}S_{2.40}Sb_{1.44}Te_{0.60}$ (Fig. 1 - 4), was revealed some anomalous behavior. First of all in the increase portions of relaxation curves, the photocurrent passes through a maximum before the stationary state is reached. Secondly, the photocurrent rises up to the maximum and then settles down to steady-state as a power function of time with the exponents, which are determined by the parameters of the localized state energy distribution [12]. These features depend on the composition of amorphous material, polarity of the applied voltage, wavelength excitation, and light intensity. In spite of the previous results, obtained for As_2S_3 , As-S-Se and As-Se amorphous thin films [9, 13, 14], on the relaxation curves of transitory photocurrents we observe another anomalous. The negative and positive spikes after

the light is switching off, depending on the composition of amorphous film, wavelength and light intensity (Fig. 1 - 4). The negative transient photocurrents were observed and investigated in amorphous films of vitreous composition $_{0.55}\text{As}_2\text{S}_3\text{:}_{0.45}\text{Sb}_2\text{S}_3$ in time-of-flight experiments [17]. The obtained experimental results have been interpreted in framework of the theoretical model, which assume that the electronic transport is controlled by trapping processes and that the dipole moments of filled traps become different from those of empty traps. This difference contributes an additional to the displacement current which may be negative in a certain time interval.

Among other things, the band gap value was estimated by the photoelectric method for the above mentioned studied samples and is about $E_g = 1.41$ eV.

3. Conclusions

The spectral distribution of steady-state photocurrent $I_{ph}(\lambda)$ and the relaxation curves of photocurrent $I_{ph}(t)$ of the amorphous thin films $\text{As}_{1.17}\text{S}_{2.7}\text{Sb}_{0.83}\text{Te}_{0.40}$, $\text{As}_{1.04}\text{S}_{2.4}\text{Sb}_{0.96}\text{Te}_{0.60}$, $\text{As}_{0.63}\text{S}_{2.7}\text{Sb}_{1.37}\text{Te}_{0.30}$, and $\text{As}_{0.56}\text{S}_{2.4}\text{Sb}_{1.44}\text{Te}_{0.60}$ in the region of wavelengths $\lambda = 0.40 \div 1.0$ μm ($3.1 \div 1.0$ eV) at positive and negative polarity of the applied voltage to the top Al illuminated electrode have been obtained and investigated. The photocurrent characteristics were registered at different wavelengths and light intensities. In all investigated amorphous thin films some maximums were revealed and are associated with the presence of the binary clusters As_2S_3 , Sb_2S_3 and Sb_2S_3 .

The relaxation curves of the photocurrent $I_{ph}(t)$ at different wavelengths and light intensities are usually typical for amorphous semiconductors, when the photocurrent increases to a maximum value and then stabilizes as a power function of time with an exponent, which are determined by the parameters of the energy distribution of the localized state. Some anomalous in the relaxation curves was observed after the light is turned off, so called negative photocurrents. It also was estimated the band gap value by the photoelectric method for the studied samples and is about $E_g = 1.41$ eV.

Acknowledgments

The authors also express their gratitude to Dr. V. Verlain and O. Bordian for their assistance in preparing experimental samples of thin films.

References

- [1] M. Popescu, A. Andriesh, V. Ciumash, M. Iovu, S. Shutov, D. Tsiuleanu, Physics of chalcogenide glasses, Ed. Bucuresti, Stiinta, in Romanian, 487 (1996).
- [2] D. Tsiuleanu, M. Ciobanu, Sensors and Actuators B, 223, 95 (2016); <https://doi.org/10.1016/j.snb.2015.09.038>
- [3] E.I. Kamitsos, J.A. Kapoutsis, I.P. Culeac, M.S. Iovu, J. Phys. Chem. B, 101, 11061 (1997); <https://doi.org/10.1021/jp972348v>
- [4] Indu Rajput, Sumesh Rana, Rudra Prasad Jena, Archana Lakhant, AIP Conf. Proc., 2100, (2019); <https://doi.org/10.1063/1.5098624>
- [5] B.M. Dally, N. Kouame, D. Houphouer-Boigny, Chalcogenide Letters 18 (11), 681 (2021); <https://doi.org/10.15251/CL.2021.1811.681>
- [6] K.A. Aly, A.M. Abouschly, A.A. Othman, J. Non-Cryst. Solids 354, 915 (2008).
- [7] O. Iaseniuc, M. Iovu, Chalcogenide Letters 19(2), 117 (2022); <https://doi.org/10.15251/CL.2022.192.117>
- [8] O. Iaseniuc, M. Iovu, S. Rosoiu, et al., Chalcogenide Letters 19(11), 841 (2022); <https://doi.org/10.15251/CL.2022.1911.841>

- [9] O. Iaseniuc, M. Iovu., Rom. Rep. Phys., 69(3), 505 (2017).
- [10] O. Iaseniuc, M. Iovu. Photoconductivity of chalcogenide thin film heterostructures. Proceedings of the Romanian Academy, ser. A, 31(3), 231 (2020).
- [11] M.A. Iovu, M.S. Iovu, S.D. Shutov., JTF Letters, 4, 1246 (1978).
- [12] A.M. Andriesh, V.I. Arkhipov, M.S. Iovu, A.I. Rudenko, S.D. Shutov, Solid State Communications, 48(12), 1041 (1983); [https://doi.org/10.1016/0038-1098\(83\)90827-X](https://doi.org/10.1016/0038-1098(83)90827-X)
- [13] M.S. Iovu, E.P. Kolomeiko, S.D. Shutov., Semiconductors, 31(7), 710 (1997).
<https://doi.org/10.1134/1.1187073>
- [14] M.S. Iovu, S.D. Shutov, V.I. Arkhipov, G.J. Adriaenssens, J. of Non-Cryst. Solids 299-302, 1008 (2002); [https://doi.org/10.1016/S0022-3093\(01\)01067-5](https://doi.org/10.1016/S0022-3093(01)01067-5)
- [15] M.A. Iovu, M.S. Iovu, S.D. Shutov, E.P. Colomeico, S.Z. Rebeja, Optoelectronics and Advanced Materials, 3(2), 473 (2001).
- [16] O. Iaseniuc, M. Iovu, Rom. J. of Phys, 62, 1 (2017).
- [17] V.I. Arkhipov, M.A. Iovu, M.S. Iovu, A.I. Rudenko, S.D. Shutov. J. Electronics, 51(6), 735 (1981); <https://doi.org/10.1080/00207218108901378>